of figure 2 are the same as those obtained by any of the manual methods commonly employed; discrepancies with respect to results obtained manually by the F/ϵ_0 method are within 5%; this was satisfactory for our purposes but it can be bettered with the use of precision analogue circuitry, which is commercially available but expensive.

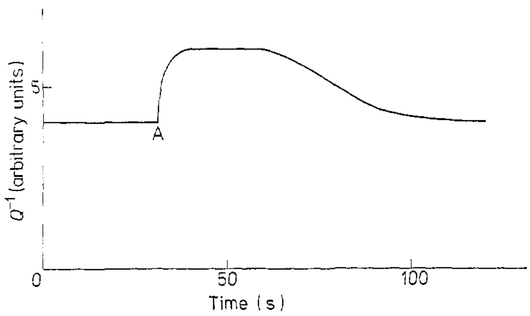

Figure 4 System response to a Q^{-1} step function; at point A a sudden introduction of air takes place, followed by a slow return to the initial conditions.

Figure 4 shows the response of the apparatus to a Q^{-1} step function, obtained by a sudden introduction of air into the vacuum chamber. The rise time of the Q^{-1} step obtained is unknown, but the curve shows that the response time of the apparatus is better than 4 s.

Acknowledgment

This work was supported by GNSM of CNR.

References

Beshers D N 1976 Internal friction
Techniques of Metals Research vol VII Part 2
ed R F Bunsham (New York: Wiley) chap. 10, pp 558, 647

Bortolotti A, Martinelli G and Passari L 1975 Amplitude-dependent internal friction in Zn monocrystals
Internal Friction and Ultrasonic Attenuation in Crystalline Solids vol II ed D Lenz and K Lücke (Berlin: Springer) p 507

Graeme J G 1973 *Applications of Operational Amplifiers: Third Generation Techniques* (New York: McGraw-Hill) p 102

Granato A and Lücke K 1956 Theory of mechanical damping due to dislocations
J. Appl. Phys. **27** 583

Lloyd A G 1971 Phase-detector/modulator operates from DC to 30 kHz
Electron. Design **12** 82

Nowick A S and Berry B S 1972 *Anelastic Relaxation in Crystalline Solids* (New York: Academic) p 427

Nuovo M 1961 Mesures dynamiques de constantes élastiques et anélastiques
Ricerca Sci. **31** 212

Tobey G E, Graeme J G and Huelsman L P (eds) 1971
Operational Amplifiers: Design and Applications (New York: McGraw-Hill) p 275

Vander Kooi M K 1973 *Linear Applications* (Santa Clara, California: National Semiconductor Corp.) pp LB 8-2, AN 31-19

J. Phys. E: Sci. Instrum., Vol. 11, 1978. Printed in Great Britain

Time resolution of a p–i–n photodiode applied as electron detector

B Jurgens, P H de Haan and H J Hopman
FOM-Instituut voor Atoom- en Molecuulfysica, Kruislaan 407, Amsterdam/Wgm, The Netherlands

Received 8 February 1978, in final form 25 May 1978

Abstract The note discusses the time resolution of p–i–n photodiodes applied as electron detectors. The rise time was found to be of the order of 1 ns, which is equal to that in the case of photon detection. However, it appears that in electron detection the initially fast decay turns over in an exponential decay with a time constant of about 30 ns. A simple algorithm is presented that corrects the recorded waveform for the effects of this tail.

1 Introduction

In a study of plasma heating by an electron beam (Jurgens *et al* 1976) a 500 keV, 500 A, 20 ns pulsed relativistic electron beam (REB) is injected into a preformed plasma. The determination of the energy distribution of the beam is a valuable tool for investigating the processes involved in the energy transfer from an REB to a plasma. To this end we developed a 180° magnetic energy analyser capable of measuring the time-resolved energy distribution of a small part of the electron beam in the range 100–750 keV. In this device p–i–n photodiodes (type Monsanto MD2) are applied as fast electron detectors. The lenses are removed to allow the electrons to hit the chip directly. In this way they are used as a kind of surface barrier detector. It has been shown that the output current of a p–i–n diode is linear with the incident current density, while the sensitivity of 9 mA mA^{-1} cm^2, corresponding to a current gain of about 1500, is nearly constant for electron energies in the range of 100–600 keV (Jurgens *et al* 1975). To obtain the energy distribution of the electron beam in the experiment the p–i–n diode detector signals are recorded in the energy analyser during 100 ns at a number of preselected energies (Jurgens *et al* 1977).

2 Experimental results

Figure 1 shows three examples of p–i–n diode signals taken in the analyser at three different energies. The beam was injected into vacuum. The beam energy loss due to the self-inductance of the system ($L\,dI_{beam}/dt$) was estimated to be less than 30 keV in this experiment. Therefore the energy of the beam electrons is approximately equal to the voltage applied to the field emission diode in which the beam electrons are accelerated. Figure 2 shows the voltage across the field emission diode as a function of time. From figure 2 it is clear that a particular electron energy will appear twice in the course of time, except for the maximum voltage. The diode signals should therefore consist of two narrow spikes. However, the data of figure 1 exhibit a substantial broadening of the spikes. The diode signals show a fast rise time, of the order of 1 ns. The decay of the signal is initially fast, but it turns over in a 'tail' having a more or less exponential decay with a time constant of about 30 ns. This tail does not correspond to the true time behaviour of the

0022-3735/78/0012-1161 $01.00

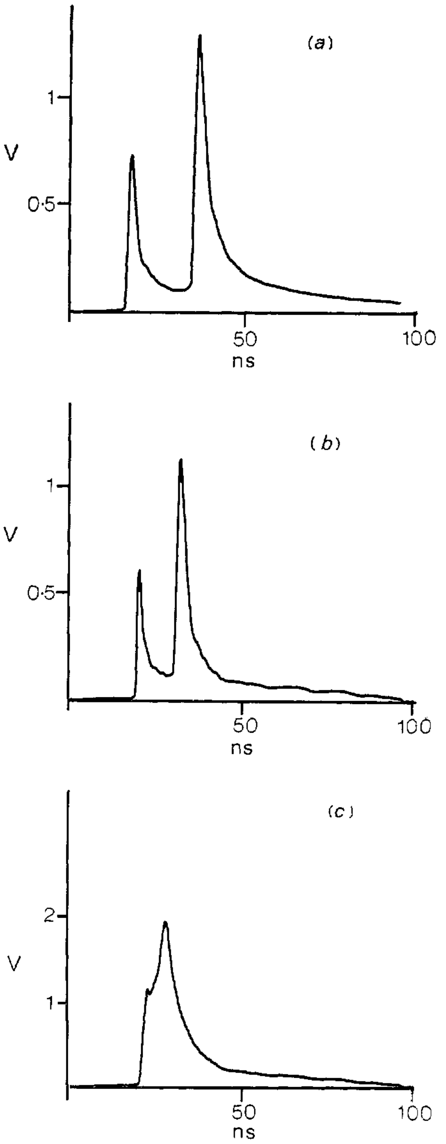

Figure 1 Signals obtained from p–i–n diode detectors in the magnetic energy analyser. The output signals are shown for three different energies: (*a*) 300 keV, (*b*) 430 keV, (*c*) 500 keV. The beam is shot into vacuum.

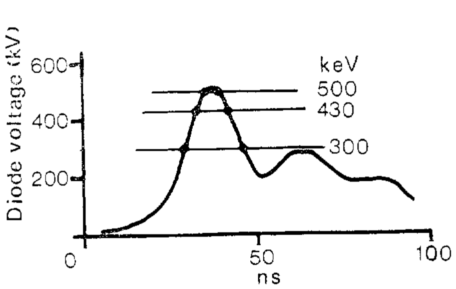

Figure 2 Voltage across the field emission diode in which beam electrons are accelerated. Horizontal levels indicate the energies corresponding to the analyser signals of figure 1.

electron current as is shown by an experiment in which the diode is exposed to a short pulse of electrons with a known current–time dependence.

In figure 3 the electron beam current registered in a metal Faraday cup is compared with the p–i–n diode response.

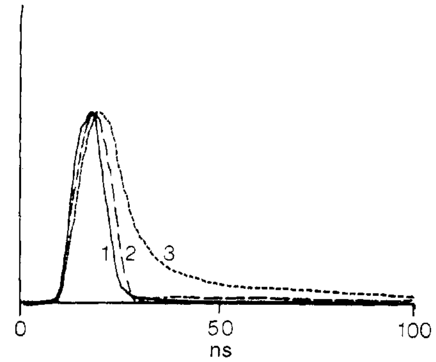

Figure 3 Response (trace 3) of the p–i–n diode to a short electron beam pulse (trace 1), and the diode signals after processing (trace 2) by the correction procedure described. All traces have been normalised to the same amplitude.

The short electron pulse in this case is produced by passing the beam through a 'filter' of 0·45 mm thick aluminium, which has a high transmittance for electrons above 400 keV only. The diode signal shows indeed the long 'tail'. The tail is not caused by the electronic circuit behind the diode, which was investigated with a 4 ns laser pulse. If we create with the laser a p–i–n (photo)diode signal of equal magnitude as observed in electron excitation, the shape of the diode signal is congruent with the shape of the light pulse. Furthermore the existence of the tail does not depend on the signal amplitude.

3 Correction of the tail

The tail exhibited by the p–i–n diode detector signals is evidently due to excitation by high-energy electrons. The tail causes an erroneous result in the measured energy distribution. Therefore we had to correct the measured signals before constructing the energy distribution from them. We now describe the procedure used for this correction.

In our experiment the signals are recorded and digitised by a Tektronix R7912 transient digitiser. This instrument gives the output of the diode detector as a function of time in $N=512$ samples over a certain period. A signal $s(t_i)$, $i=1, 2, \ldots, N$, is obtained where $t_i=i\Delta t$. A corrected signal $\bar{s}$ is calculated (by a minicomputer) according to an empirical formula,

$$\bar{s}(t_i)=s(t_i)-\nu_1\sum_{k=1}^{i-1}\exp\left[-(t_{i-1}-t_k)/\tau_1\right]s(t_k)\Delta t$$
$$+\nu_2\sum_{k=1}^{i-1}\exp\left[-(t_{i-1}-t_k)/\tau_2\right]s^2(t_k)\Delta t \qquad (1)$$

where ν_1, τ_1, ν_2, τ_2 are constants which have been adjusted such that the tail of the diode signal is optimally reduced (see figure 3). Optimum values are $\nu_1=4{\cdot}3\times10^8\ \mathrm{s}^{-1}$, $\tau_1=1{\cdot}9$ ns, $\nu_2=7{\cdot}7\times10^5\ \mathrm{s}^{-1}$, $\tau_2=1{\cdot}2$ ns for the diode used, which has a decay time of the tail $\tau=30$ ns. The result of applying equation (1) to an actual measurement is presented in figure 4.

4 Discussion

The effect of the correction procedure can be illustrated by applying it to an idealised signal. The response of the diode to a δ-function electron pulse can be approximated by

$$s(t)=s_0\exp(-t/\tau), \qquad t\geq 0 \qquad (2)$$

where τ is the time constant of the exponentially decaying

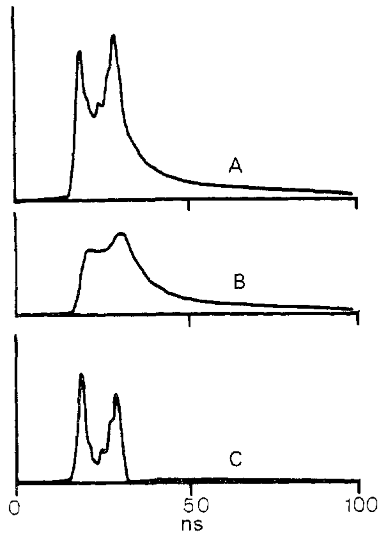

Figure 4 Correction of the p–i–n diode signal: A, original signal; B, correction; C, corrected signal = A − B. All on the same (arbitrary) scale.

tail. Applying only a linear correction, according to equation (1) we have in the limit $\Delta t \to 0$

$$\bar{s}(t) = s_0 \exp(-t/\tau) - s_0 \nu_1 \int_0^t \exp[-(t-t')/\tau_1] \exp(-t'/\tau)\,\mathrm{d}t', \quad (3)$$

and by integration

$$\bar{s}(t) = s_0 \exp(-t/\tau)\{1 - \nu_1\tau^*[1 - \exp(-t/\tau^*)]\}, \quad (4)$$

where $1/\tau^* = -1/\tau + 1/\tau_1$. The correction $\nu_1\tau^*[1 - \exp(-t/\tau^*)]$ is zero for $t = 0$ and approaches $\nu_1\tau^*$ for $t \to \infty$, if we choose $\tau_1 < \tau$ such that $\tau^* > 0$. If we further choose ν such that $\nu\tau^* = 1$, equation (3) reduces to

$$\bar{s}(t) = s_0 \exp(-t/\tau_1), \quad (5)$$

so our new signal decays with a time constant $\tau_1 < \tau$. Since the actual signals deviate from the idealised exponential decay, the optimum value of ν_1 is such that $\nu_1\tau^* = 0{\cdot}86 \neq 1$. The actual signals also contain a fast decaying part, as can be seen in figure 1. This part also contributes to the correction, which therefore tends to be too large at small times. So we introduced a quadratic, faster decaying, positive correction term in equation (1). The constants ν_2 and ν_1 are adjusted to keep the corrected signal positive for smaller times.

The ratio of the sum over the samples of the corrected signal to the sum over the original signal does not depend on the time dependence of the signal. For 100 measured p–i–n diode signals of very different time dependence (see e.g. figure 1), we find

$$\frac{\sum_{i=1}^{512} \bar{s}(t_i)}{\sum_{i=1}^{512} s(t_i)} = 0{\cdot}3 \pm 10\%. \quad (6)$$

The signals to be processed by this method consist in general of two subsequent pulses, as can be seen in figures 1 and 4. The first correction term of equation (1) is linear and thus there is no interference between the two signals – they just add. By nature of the p–i–n diode both pulses have the same decay constant. The second quadratic correction term is not additive and gives a contribution from the cross-product of the two pulses. However, this is a small term as long as the second pulse does not follow the first one within $3\tau_2$. In addition the quadratic term causes the correction to be amplitude-dependent, so it is advisable to normalise the signals at first. In our experiment this has been done roughly by adjusting the sensitivity of the transient digitiser.

In the program used in the minicomputer of the experiment we made the substitution

$$\begin{aligned} c_1(i) &= p_1 c_1(i-1) + q_1 s(t_i) \\ c_2(i) &= p_2 c_2(i-1) + q_2 s^2(t_i) \\ \bar{s}(t_i) &= s(t_i) - c_1(i) + c_2(i) \end{aligned} \quad (7)$$

where $q_{1,2} = \nu_{1,2}\Delta t$ and $p_{1,2} = \exp(-\Delta t/\tau_{1,2})$. With the new expressions, it takes only $5N + 7$ executions of FORTRAN statements to perform the correction.

5 Conclusion

At low electron current levels p–i–n diodes have been found to be useful detectors in a magnetic energy analyser. They show a fast rise time of 1 ns, but the decay which is initially also fast turns over in a 'tail' decaying with a time constant of about 30 ns. The time resolution of the energy distribution obtained with the analyser is improved by a simple *ad hoc* correction procedure applied to the diode signals. With this correction details in the energy distribution are shown with a time resolution of about 3 ns. The correction procedure is very suitable for use with a minicomputer or microprocessor. It can be used to improve digitised signals showing an artificial exponential decay which is much longer than the rise time. Such occurs, e.g. in semiconductor detectors or scintillators. Since the procedure depends only on previous samples it might also be applied to continuously sampled signals.

Acknowledgments

The authors thank Dr E H A Granneman for valuable discussions. This work was performed as a part of the research program of the association agreement of EURATOM and the Stichting voor Fundamenteel Onderzoek der Materie (FOM), with financial support from the Nederlandse Organisatie voor Zuiver-Wetenschappelijk Onderzoek (ZWO) and EURATOM.

References

Jurgens B, de Haan P H, Hopman H J and de Jagher P C 1977 Energy distribution of a relativistic electron beam interacting with plasma
Phys. Rev. Lett. **39** 936

Jurgens B, Hopman H J, de Haan P H, de Jagher P C and Kistemaker J 1976 Energy transfer of a relativistic electron beam to a plasma
Proc. 6th Int. Conf. on Plasma Physics and Controlled Nuclear Fusion Research, Berchtesgaden p G2–1: *Nucl. Fusion* Suppl. 1977

Jurgens B, Vijftigschild A, Vrijdaghs J B and Hopman H J 1975 Application of a p–i–n photodiode as a low current electron detector with nanosecond time resolution
J. Phys. E: Sci. Instrum. **8** 629